Analytica Chimica Acta 1166 (2021) 338573

Contents lists available at ScienceDirect

Analytica Chimica Acta

journal homepage: www.elsevier.com/locate/aca

Enhancement of acidic lipid analysis by nanoflow ultrahigh performance liquid chromatography–mass spectrometry

Jong Cheol Lee , Young Beom Kim , Myeong Hee Moon *

Department of Chemistry, Yonsei University, 50 Yonsei-ro, Seodaemun-gu, Seoul, 03722, South Korea

HIGHLIGHTS

- Acidic lipid analysis by nUHPLC-ESI-MS/MS was enhanced with carbamate-embedded C18.
- Tailing factor and time-based separation efficiency were used for optimisation.
- The number of identified acidic lipids increased by ~30% with the optimised method.
- Quantification efficiency was validated with acidic/other lipid-spiked plasma SRM.

GRAPHICAL ABSTRACT

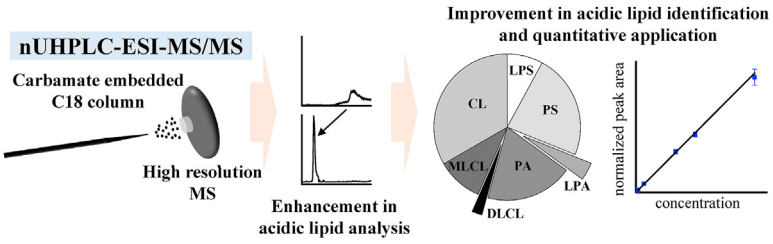

ARTICLE INFO

Article history:
Received 18 February 2021
Received in revised form
31 March 2021
Accepted 22 April 2021
Available online 27 April 2021

Keywords:
Acidic lipid
Lipidomics
Nanoflow UHPLC
Mass spectrometry
Validation
Porcine brain lipids

ABSTRACT

Acidic lipids are associated with the regulation of the structure and function of membrane proteins. Therefore, accurate and highly precise analysis of acidic lipids is important for elucidating their biological roles and pathological mechanisms. In this study, an enhanced analytical method for the separation and quantification of acidic lipids, including phosphatidylserine (PS), phosphatidic acid (PA), cardiolipin, and their lyso-derivatives, was developed using nanoflow ultrahigh performance liquid chromatography–electrospray ionisation-tandem mass spectrometry. The separation and mass spectrometry detection of acidic lipids were optimised in terms of peak tailing and time-based separation efficiencies, with carbamate-embedded C18 as the stationary phase, in the presence of an appropriate liquid chromatography solvent modifier. This newly developed method was applied to analyse a lipid extract from porcine brain. A significant increase in the number of acidic lipids identified (176 vs. 134), including intact monolysocardiolipin (17 vs. 4), was observed with the new method compared with conventional C18. The quantification of acidic lipids was validated with plasma standard (NIST SRM 1950) spiked with a number of LPS and PS standards, and acceptable accuracy (<15%) was obtained. The present method was found to be reliable for the acidic lipid analysis based on qualitative results from tissue extract and plasma samples.

1. Introduction

Lipids are essential molecules in biological systems that make up the cellular membrane structures. In addition, they play important roles in signal transduction, cell proliferation, and apoptosis [1,2]. Lipids are classified into eight categories, namely glycerophospholipids (GPs), glycerolipids, sphingolipids, sterols, fatty acids, prenols, saccharolipids, and polyketides. GPs (or simply phospholipids), which are key components in the cell bilayer

* Corresponding author.
E-mail address: mhmoon@yonsei.ac.kr (M.H. Moon).

https://doi.org/10.1016/j.aca.2021.338573
0003-2670/

Abbreviations

BEH	ethylene bridged hybrid
Cer	ceramide
CL	cardiolipin
CE	cholesteryl ester
DG	diacylglycerol
DLCL	dilysocardiolipin
EIC	extracted ion chromatogram
FA	fatty acid
GP	glycerophospholipid
GL	glycerolipid
HexCer	monohexosylceramide
Hex2Cer	dihexosylceramide
IPA	isopropanol
LPS	lysophosphatidylserine
LPA	lysophosphatidic acid
LPC	lysophosphatidylcholine
LPE	lysophosphatidylethanolamine
LPG	lysophosphatidylglycerol
LPI	lysophosphatidylinositol
LSM	lysosphingomyelin
LLOQ	lower limit of quantitation
MLCL	monolysocardiolipin
MG	monoacylglycerol
MS	mass spectrometry
MS/MS	tandem MS
MTBE	methyl-*tert*-buthyl ether
MMC	(MeOH, MTBE, and $CHCl_3$)
N/t_r	retention time based plate number
nUHPLC	nanoflow ultrahigh performance liquid chromatography
PCA	principal component analysis
PS	phosphatidylserine
PA	phosphatidic acid
PC	phosphatidylcholine
PE	phosphatidylethanolamine
PG	phosphatidylglycerol
PI	phosphatidylinositol
PC-P	plasmenyl PC
PE-P	plasmenyl PE
RPLC	reversed phase LC
SP	sphingolipid
SM	sphingomyelin
SulfoHexCer	sulfatide
TG	triacylglycerol
T_f	tailing factor

structures, share a glycerol-3-phosphate backbone with two hydroxyl groups esterified by fatty acids and with its phosphate group accompanied by various head groups. Depending on the type of head group and pH conditions, some of the GPs may be classified as anionic lipids, examples of which include phosphatidylglycerol (PG), phosphatidylinositol (PI), phosphatidylserine (PS), phosphatidic acid (PA), and cardiolipin (CL). Among the anionic lipids, PS, PA, CL, lysophosphatidylserine (LPS), lysophosphatidic acid (LPA), monolysocardiolipin (MLCL), and dilysocardiolipin (DLCL) are acidic because they can carry two negative charges. While PA has two charged sites on a single phosphate group and CL has two charged sites on two phosphate groups bridged by glycerol, PS has one charged site in the phosphate group and another in the carboxyl group of serine, however its charge status is not favorably -2 at physiological pH and rather between single and double anionic structure. Owing to their deprotonation capability, acidic lipids are distinct compared to other anionic lipids such as PG and PI in terms of structural characteristics, and they play important functional roles in biological systems [3–5]. Acidic lipids can regulate the structure and function of membrane proteins by participating in specific lipid-protein bindings or non-specific electrostatic interactions [6,7]. It is reported that the negative charge of PA is -1 at pH 7.0 and it increase to -2 when it interacts with lysine or arginine, which stabilizes protein-lipid interactions [8]. In addition, PA can influence membrane rearrangement by forming negative membrane curvature as well as by membrane fusion and fission [9]. PS is enriched in the cytosolic side of the plasma membrane under normal physiological conditions, while it is exposed on the outer side of the membrane during apoptosis. This is a well-known example of non-specific electrostatic interactions. Thus, PS and PA are thought to be involved in binding to specific proteins and in modulating the structural and functional characteristics of membrane proteins [10,11].

Lipid analyses have mostly been conducted using mass spectrometry (MS). MS-based lipid analyses are generally carried out by the direct infusion of lipidome samples or chromatographic interfaces, such as by employing liquid chromatography (LC) prior to MS. As LC–MS-based approaches offer several advantages such as the reduction of ion suppression effect induced by abundant ions and the separation of regioisomers or structural isomers [12,13], they are widely used with normal phase LC (NPLC) [14], reversed-phase LC (RPLC) [15], and hydrophilic interaction LC (HILIC) [16]. In both NPLC and HILIC, lipid separation relies on the affinity of the lipid to a polar stationary phase. Consequently, lipids are separated by their polar head groups. Although some HILIC-based lipidomic methods with complicated optimisation steps have been developed to analyse acidic lipids [17,18], there are limitations in comprehensively analysing a variety of lipid molecules with various fatty acid chains. In contrast, lipid separation by RPLC relies on the hydrophobic interactions between the lipid molecules and non-polar stationary phase. This allows comprehensive separation of lipids based on differences in the chain length, degree of unsaturation, type of polar head groups, and isomeric lipid structures. While sophisticated RPLC–MS methods have been developed for high-speed and high-throughput analysis of complicated lipid mixtures with biological origins, the analysis of acidic lipids such as PA, PS, CL, and their lyso-derivatives still needs to be improved due to the poor separation of negatively charged lipids when multiple lipid classes need to be simultaneously analysed. To overcome the limitations in analysing acidic lipids with RPLC, a few attempts have been made to add phosphoric acid to the mobile phase as a solvent modifier [19,20] or directly to the lipid extract sample for supplementation [21]. However, enhancing acidic lipid analysis has not been thoroughly examined so far.

In this study, we investigated the efficiency of analysing acidic lipids by using two different packing materials with varying the concentration of LC solvent modifiers (NH_4HCO_2, NH_4OH, and H_3PO_4) in nanoflow ultrahigh performance LC–electrospray ionisation-tandem mass spectrometry (nUHPLC–ESI-MS/MS). The incorporation of a capillary column with UHPLC in the nanoflow regime facilitated lipidomic analysis with high-resolution separation of lipids and substantial reduction in the lipid amounts required for analysis as well as increased MS sensitivity [22,23]. In our laboratory, nUHPLC–ESI-MS/MS has been applied to study

lipidomic perturbations in various biological samples such as plasma from cancer patients [24], muscle tissue from high-fat diet-induced mice [25], and subcellular organelles with exosomes from oxidatively stressed cell lines [26]. For optimising the acidic lipid analysis, the performances of two variants of ethylene-bridged hybrid C18 particles in the nUHPLC–ESI-MS/MS analysis were evaluated by comparing the tailing factors and time-based separation efficiencies of acidic lipid standards containing various solvent modifier concentrations. In addition, the number of acidic lipids identified in a porcine brain lipid extract were also compared for the two hybrid C18 particles. An optimised method was validated by spiking National Institute of Standards and Technology (NIST) Standard Reference Material (SRM) 1950 plasma samples with 81 external lipid standards and a mixture of 24 internal lipid standards [27].

2. Experimental

2.1. Materials and reagents

All the lipid standards were purchased from Avanti Polar Lipids Inc. (Alabaster, AL, USA; LPS 18:1, PS 16:0/16:0, PS 18:0/18:0, LPA 18:0, PA 12:0/12:0, PA 14:0/14:0, PA 16:0/22:6, PA 16:0/18:1, PA 18:0/18:0, DLCL $(18:2)_2$ (bovine heart extract), MLCL $(18:2)_3$ (bovine heart extract), CL $(14:0)_4$, and CL $(18:1)_4$). A total lipid extract of porcine brain was purchased from Avanti Polar Lipids Inc. (Alabaster, AL, USA) and NIST SRM 1950 plasma was purchased from the National Institute of Standards and Technology (Maryland, USA). For the precision and accuracy tests, an external standard lipid mixture was prepared by mixing 25 standard lipids having odd fatty acid chains or deuterium-labeled moieties with UltimateSPLASH™ ONE from Avanti Polar Lipids Inc. The details of this mixture are listed in Table S1. An internal standard lipid mixture was prepared using SPLASH® LIPIDOMIX® by adding 11 additional standards (FA 15:0, LPG 13:0, LPI 13:0, LPS 13:0, LPA 17:1, CL $(14:0)_4$, Cer d18:1-d_7/24:0, LSM d17:1, HexCer d18:1-d_7/15:0, Hex2Cer d18:1-d_7/15:0, and SulfoHexCer d18:1-d_7/13:0) in order to compensate for the deficient lipid classes, as listed in Table S2. Since the lipid solvent compositions can affect the lipidomic results, the external and internal standard lipid mixtures contained only $CHCl_3$ and methanol (MeOH), respectively, as solvents. HPLC grade solvents (H_2O, CH_3CN, CH_3OH, isopropanol (IPA), and methyl-*tert*-butyl ether (MTBE)) were purchased from Avantor Performance Materials (Center Valley, PA, USA). NH_4HCO_2, NH_4OH, H_3PO_4, and $CHCl_3$ were purchased from Sigma-Aldrich (St. Louis, MO, USA). Fused silica capillary tubes with inner and outer diameters of 100 and 360 μm, respectively, were purchased from Polymicro Technology, LLC (Phoenix, AZ, USA). The packing materials used to prepare capillary columns were ethylene-bridged hybrid (BEH) C18 (1.7 μm and 130 Å) and BEH Shield C18 particles (1.7 μm and 130 Å), both of which were unpacked from the ACQUITY UPLC BEH C18 column (2.1 mm × 100 mm) and ACQUITY UPLC BEH Shield RP18 column (2.1 mm × 100 mm), respectively. These were purchased from Waters (Milford, MA, USA). The BEH Shield RP18 particles were embedded with carbamate. Watchers ODS-P C18 particles (3 μm and 100 Å) from Isu Industry Corporation (Seoul, Korea) were used to fabricate the self-assembled frit (~5 mm) at the tip of the analytical columns prior to packing with 1.7 μm C18 particles. Pierce™ LTQ Velos ESI Positive Ion Calibration Solution and Pierce™ Negative Ion Calibration Solution were purchased from Thermo Scientific (San Jose, CA, USA).

2.2. Lipid extraction

For the analysis of the external or internal lipid standard mixtures, the standard plasma samples were spiked with standard mixtures. To measure extraction recovery, an internal standard mixture (10 μL) was added to the NIST SRM 1950 plasma sample (10 μL), and the sample was spiked with the external standard mixture (10 μL) before or after extraction. For two-phase lipid extraction, 1300 μL of MTBE/MeOH mixture (10:3, v/v) was added to the sample, and mixed with a vortex shaker for 60 min at 40 °C. Subsequently, 250 μL of H_2O was added to the mixture. The mixture was then shaken with a vortex shaker for 10 min and centrifuged for an additional 10 min at 16000*g*. After the upper organic layer was removed, 400 μL of MTBE was added to the remaining lower aqueous layer. This solution was then vortexed for 10 min at 40 °C and centrifuged. The resulting organic layer was mixed with the previously collected organic solution containing the lipid extract. For one-phase lipid extraction, 1300 μL of MeOH/MTBE/$CHCl_3$ (1.33:1:1, v/v/v) was added to the plasma sample. The mixture was vortexed for 10 min at 40 °C, followed by centrifugation at 16000*g* for 10 min. The organic supernatant was then removed. The organic solutions collected in both the extraction protocols were dried under N_2 gas using an Evatros mini evaporator from Goojung Engineering (Seoul, Korea) and dissolved in 200 μL of MeOH/$CHCl_3$/H_2O (8.5:0.5:1, v/v/v). This solvent composition and volume were used for dissolving lipid extracts from the plasma samples for all the subsequent experiments. For the method validation experiments, the one-phase lipid extraction protocol was applied.

2.3. nUHPLC–ESI-MS^n

For the identification and quantification of lipids, an nUHPLC–ESI-MS system was utilised with a Dionex Ultimate 3000 RSLCnano system equipped with a Q Exactive mass spectrometer (Thermo Scientific, San Jose, CA, USA) via Nanospray Flex™ Ion Source for nanoflow ESI. ESI-MS system was regularly calibrated with positive and negative ion calibration solutions. To set up the nUHPLC system with minimised dwell time, nanoViper capillaries (20 μm inner diameter) with customised lengths from Thermo Scientific were used for all the connections. The capillaries were used to connect the UHPLC pump outlet to the injection valve of an autosampler (550 mm long) and the injection valve to a MicroTee (850 mm long). The other two ports of the MicroTee were connected to a Pt wire (for ESI voltage) as well as to an analytical column. Since the dead volume of MicroTee was 152 nL and volume of the sample loop was 1 μL, the resulting dead volume for the nUHPLC system was approximately 1623 nL.

The analytical column was prepared in our laboratory with a silica capillary (100 μm inner diameter) by pulling one end with a flame to obtain a sharp tip. The sharp tip was then cut into a self-emitter for ESI. The tip (~5 mm) was filled with Watchers ODS-P C18 particles as a self-assembled frit and the remaning capillary was packed with BEH C18 or BEH Shield C18 particles using N_2 gas at 1000 psi pressure. The mobile phase solutions A and B consisted of H_2O/CH_3CN (9:1, v/v) and IPA/CH_3OH/CH_3CN/H_2O (7:1.5:1:0.5, v/v/v/v), respectively. NH_4HCO_2, NH_4OH, and H_3PO_4 were used as a solvent modifier. The UHPLC pump flow rate was set to 800 nL min^{-1}, while the injection volume was maintained as 0.2 μL for all the experiments, except in the case of the porcine brain extracts, where the injection volume was 0.5 μL. Gradient elution began with 1% of mobile phase B, which was increased to 75% for 5 min, to 90% for the next 5 min (except in the case of the porcine brain extracts, where the mobile phase B was increased to 80%, not 90%), and to 99% for another 15 min. The mobile phase B was then maintained at 99% for 5 min, following which it was decreased to 1% for 5 min, resulting in a total duration of 35 min for each nUHPLC analysis. For high-resolution MS detection of lipids, the ESI voltages for both the positive and negative ion modes were set to 3 kV and

the ion transfer tube temperature was 350 °C. For the qualitative analysis of lipids, full MS scan mode and subsequent data-dependent MS/MS acquisition were utilised in the positive and negative scan modes. The lipid molecular structures were identified using the LipidMatch software [28] and manually confirmed by considering the exact mass of the precursor ions (5 mDa tolerance), retention time, and characteristic MS/MS spectra. For the quantitative analysis of lipids, only the full MS scan mode was utilised for scanning both the positive and negative ions alternately, by the polarity switching method in a single nUHPLC run. Details of the MS parameters are described in Table S3. The data were processed using the Thermo Scientific Xcalibur software. The normalised peak area was defined as the ratio of the peak area of a lipid relative to that of its internal standard lipid. In the case of FA, the normalised peak area ratio was corrected by subtracting the blank signal [29], in order to avoid the influence of residues from the plastic vials.

2.4. Tailing factor and time-based separation efficiency

In order to evaluate the separation efficiency of acidic lipids, the time-based plate number (N/t_r) and tailing factor (T_f) were used. N/t_r was calculated as the ratio of plate number (N) to retention time (t_r), while N was measured as the ratio of $5.55t_r^2$ to the square of the full peak width at 50% of the peak height ($w_{0.5}^2$). T_f was calculated as the ratio of half of the full peak width at 5% of the peak height ($w_{0.05}/2$) to the front half width (f) at 5% of the peak height ($w_{0.05}/2f$).

2.5. Calibration curves and method validation

To construct the calibration curves, the NIST SRM 1950 plasma samples were spiked before extraction with a fixed concentration of the internal standard mixture and different concentrations of the external standard mixture. Ten microliters of each plasma sample and standard mixture were used. For each external standard concentration, five replicates of the samples were prepared and extracted. Each sample analysis was repeated three time by nUHPLC–ESI-MS. A calibration curve of normalised peak area ratio vs. nominal concentration was constructed for each lipid standard. The normalised concentration of an individual external standard lipid was calculated using a linear regression equation, which includes the lower limit of quantification (LLOQ). LLOQ is defined as the lowest concentration of an external standard lipid in a sample that falls with the accepted criteria (<20%) for the coefficient of variation (CV) of the normalised peak area ratio and accuracy [30]. Accuracy was defined as the difference in error between the nominal concentration and normalised lipid concentration.

3. Results and discussion

3.1. Optimisation of acidic lipid separation by nUHPLC–ESI-MS

The separation of acidic lipids was evaluated using a mixture of 13 acidic lipid standards including PS, PA, CL, and their lyso-derivatives, by varying the solvent modifier as well as the packing materials in the nUHPLC column. Fig. 1 compares the extracted ion chromatograms (EICs) of the standard acidic lipid mixture (0.2 pmol of each standard) obtained by nUHPLC–ESI-MS. Runs were achieved with BEH C18 with and without H_3PO_4 added to the mobile phase as solvent modifier, as well as with carbamate-embedded C18 column. A solvent modifier mixture consisting of 0.5 mM NH_4HCO_2 and 7.4 mM NH_4OH was typically used. In some cases, H_3PO_4 was added to this mixture. The acidic lipids were detected in the negative ion mode. As shown in Fig. 1a, most of the acidic lipid species except for LPA (peak 1) and LPS (peak 2) were eluted as broad peaks with peak tailing in the nUHPLC system packed with ethylene-bridged (BEH) C18 particles. When 8 μM H_3PO_4 was added to the mobile phase, as shown in Fig. 1b, most of the peaks appeared to be sharper with increased peak intensities and reduced peak tailing (especially peaks 5, 6, and 8) and retention times. These results are consistent with previous reports [19,20]. However, the separation of acidic lipids still needs to be improved because of the poor resolution (e.g., resolution of peak numbers 7 and 8) and distorted peak shapes (especially for peak 11) observed. When carbamate-embedded BEH C18 was used as the packing material and in the absence of H_3PO_4 in the mobile phase (Fig. 1c), peak tailing was significantly reduced with increase in peak resolution. In particular, PA 18:0/18:0 (peak number 11) can be detected at increased peak intensity. In order to evaluate the improvements more systematically, the tailing factor (T_f) and time-based separatoin efficiency (N/t_r) values of the acidic lipids were plotted in Fig. 2. When carbamate-embedded C18 was used as the packing material, the tailing factors of most of the acidic lipids were significantly decreased to ~1.0, supporting the peak shapes of most of the symmetric peaks. However, the PA and PS molecules still exhibited tailing, although the tailing was improved. In the case of LPA 18:0 (#1), LPS 18:1 (#2), DLCL $(18:2)_2$ (#4), and MLCL $(18:2)_3$ (#9), experimental T_f or N/t_r values could not be calculated because regioisomers of some species were not completely separated under some run conditions so that the half of full peak width at 5% or 50% of the peak height can not be calculated. The time-based separation efficiencies, represented by the N/t_r values in Fig. 2b, significantly increased with the use of polar group embedded C18 in the columns (1.16-fold for DLCL $(18:2)_2$–21.2-fold for CL $(18:1)_4$, compared with normal C18). In addition, compared to normal C18 and with 8 μM H_3PO_4 added to the mobile phases, the tailing factors and N/t_r values improved significantly, especially for PA 16:0/22:6, PA 16:0/18:1, PA 18:0/18:0, MLCL $(18:2)_3$, CL $(14:0)_4$, and CL $(18:1)_4$. Furthermore, the N/t_r value of PS 16:0/16:0 (#7) was not affected by the addition of H_3PO_4, but was improved with the carbamate-embedded C18 column. Overall, employing carbamate-embedded C18 particles was proven to be effective for acidic lipid separation with substantial reduction in analysis time (from ~27 to ~15 min for CL $(18:1)_4$). This was attributed to the decrease in the hydrophobicity of the stationary phase by the embedded polar carbamate.

For further optimising the nUHPLC–ESI-MS analysis of acidic lipids with a carbamate-embedded C18 column, the NH_4OH concentration was varied, while the NH_4HCO_2 concentration was fixed at 0.5 mM, as shown in Fig. S1. When the NH_4OH concentration was decreased from 7.4 (Figs. 1c) to 5 mM (Fig. S1b), the peak intensities increased with no significant increase in retention time. Further decrease in the NH_4OH concentration did not induce a significant change in separation up to 0.5 mM (Fig. S1c). Moreover, the addition of a small amount (8 μM) of H_3PO_4 to the mobile phases was completely ineffective for the separation of acidic lipids with the carbamate-embedded C18 column, as shown in the two chromatograms shown in Figure S1d~e. Therefore, a mixture of 5 mM NH_4OH and 0.5 mM NH_4HCO_2 was used as the solvent modifier for the carbamate-embedded C18 column.

3.2. Identification of acidic lipids in porcine brain extracts

The optimised method was applied for the analysis of acidic lipids in a total lipid extract of porcine brain by nUHPLC–ESI-MS/MS. C18 particles with or without carbamate were used for packing the columns. The brain lipid extract was dissolved in MeOH/$CHCl_3$/H_2O (8.5:1.25:0.25, v/v/v) at a concentration of 10 mg/mL. The number of identified lipids in each acidic lipid class obtained using the two columns were compared using the pie charts shown in

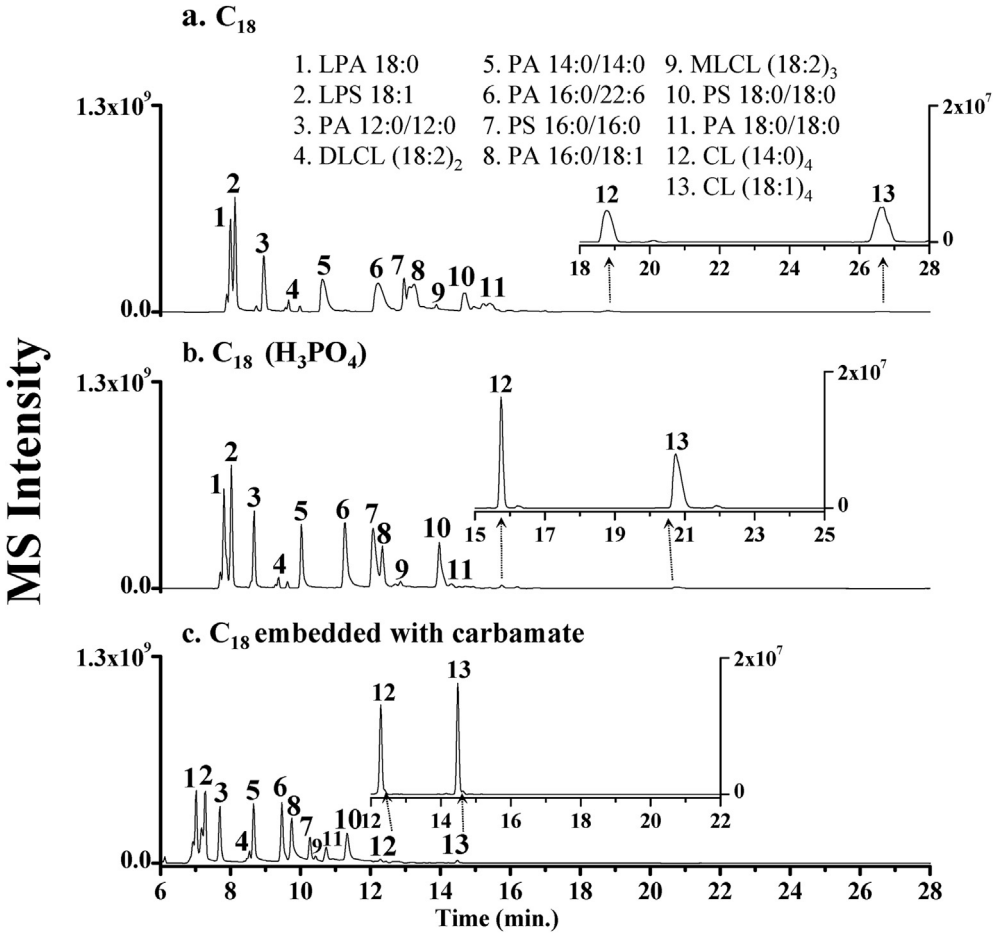

Fig. 1. Extracted ion chromatograms (EICs) of the standard acidic lipids obtained in the negative ion mode of nUHPLC–ESI-MS with columns consisting of a) ethylene-bridged C18 particles, b) ethylene-bridged C18 particles with 8 μM H_3PO_4 added as LC solvent modifier, and c) ethylene-bridged C18 particles embedded with carbamate. In all the cases, a mixture of 0.5 mM NH_4HCO_2 and 7.4 mM NH_4OH were used as the solvent modifier. *m/z* value of each standard lipid was as follows; 1. LPA 18:0 (437.267), 2. LPS 18:1 (522.284), 3. PA 12:0/12:0 (535.341), 4. DLCL $(18:2)_2$ (461.249), 5. PA 14:0/14:0 (591.403), 6. PA 16:0/22:6 (719.466), 7. PS 16:0/16:0 (734.498), 8. PA 16:0/18:1 (673.481), 9. MLCL $(18:2)_3$ (592.364), 10. PS 18:0/18:0 (790.560), 11. PA 18:0/18:0 (703.528), 12. CL $(14:0)_4$ (619.416), 13. CL $(18:1)_4$ (727.510).

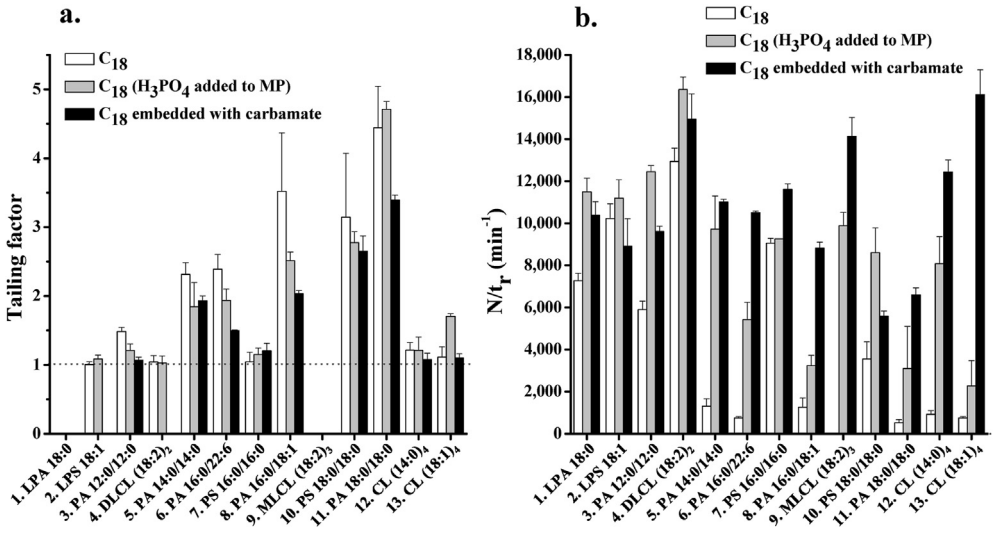

Fig. 2. a) Tailing factor (T_f) and b) time-based separation efficiency (N/t_r) of acidic lipid standards from the nUHPLC–ESI-MS results (n = 3).

Fig. 3. A total of 176 and 134 acidic lipids were identified using the method developed in this study and conventional ethylene bridged C18, respectively. Molecular structures of the identified acidic lipids between the two columns are compared in Table S4. More acidic

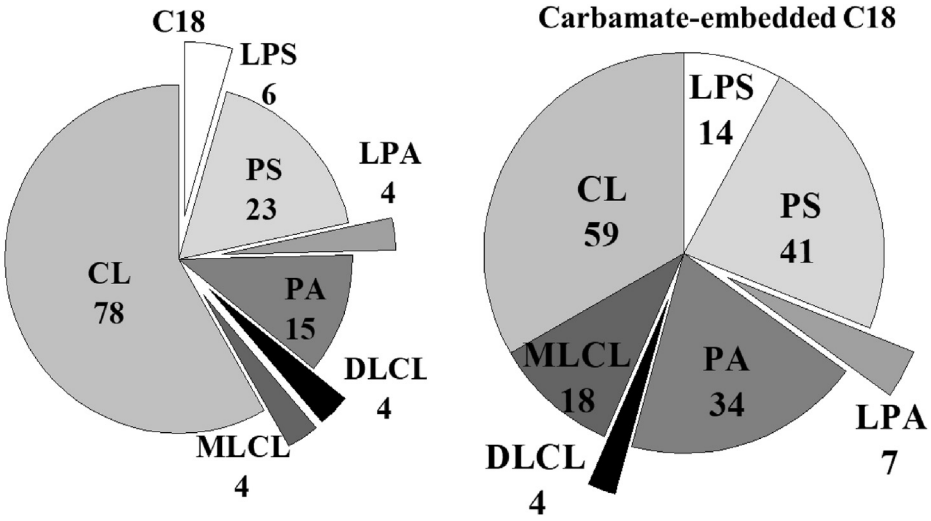

Fig. 3. Comparison of the number of acidic lipids identified from a porcine brain extract, using the two columns.

lipids were identified with the carbamate-embedded C18 column compared to the C18 column, implying that the newly developed method is effective for the acidic lipid analysis. Specifically, 8 LPS species, 18 PS, 3 LPA, 19 PA, and 13 MLCL were additionally found with the carbamate-embedded C18 column, as listed in Table S4. However, the number of CL identified decreased from 78 to 59, while those of MLCL or DLCL increased or remained the same. The reason for the poor results with CL is not clearly understood yet, but we speculate that it could be due to the increased spectral congestion caused by the fast elution of CL molecules, which are not abundant. The enhanced detection capability was illustrated in the EICs of PA 32:1 (*m/z* 645.450, from PA 14:0_18:1 and PA 16:0_16:1), FA 18:1 (*m/z* 281.249), and PI 38:4 (*m/z* 885.550, from PI 16:0_22:4 and PI 18:0_20:4), as shown in Fig. 4. The peak intensities of FA 18:1 and PI 38:4 were increased by two orders of magnitude with the carbamate-embedded C18 column. In general, the peak of a lipid species is likely to be broader for extracts from biological samples compared to standards. This phenomenon was more prominent for PA 32:1 analysed with the C18 column compared to that with the carbamate-embedded C18 column. In contrast, the FA and PI species were not significantly influenced. The magnified EIC showed other peaks at ~19 min (Fig. 4a) and ~15.5 min (Fig. 4b), which were determined to be PA 32:1 produced by the in-source fragmentation of PC 32:1 (*m/z* 645.450) during ESI. While PA 32:1 can be detected in Fig. 4a in the 13–14 min time interval, its peak intensity in Fig. 4a was about two orders of magnitude lower than that of the sharp peak in Fig. 4b. Another advantage of this method was the improved detection of the MLCL species (17 vs. 4). To the best of our knowledge, this is the largest number of MLCL species identified from raw lipid extracts without methylation of the phosphate group, which is known to enhance the ionisation efficiency of polyglycerophospholipids [31]. The MS spectra (Fig. 5a) exhibit peaks corresponding to MLCL species of 52:3, 54:5, 56:7, and 58:9 detected at t_r = 11.44 min along with their fragment ion spectra obtained from data-dependent MS/MS experiments (Fig. 5b and c). All the MS/MS spectra exhibited peaks that are characteristic of the diacylglycerol-3-phosphate fragment ion, $[DGP_f]^-$, produced by the dissociation of a central glycerol and phosphate linked to a diacylglycerol unit of MLCL (see cleavage pattern in Fig. 5). Peaks corresponding to a characteristic fragment ion at *m/z* 152.995, $[C_3H_5O_5P]^-$, representing the neutral loss (NL) of H_2O from glycerol-3-phosphate was also observed. The MS/MS spectra of MLCL 56:7 in Fig. 5b represent the higher-energy collision dissociation (HCD)

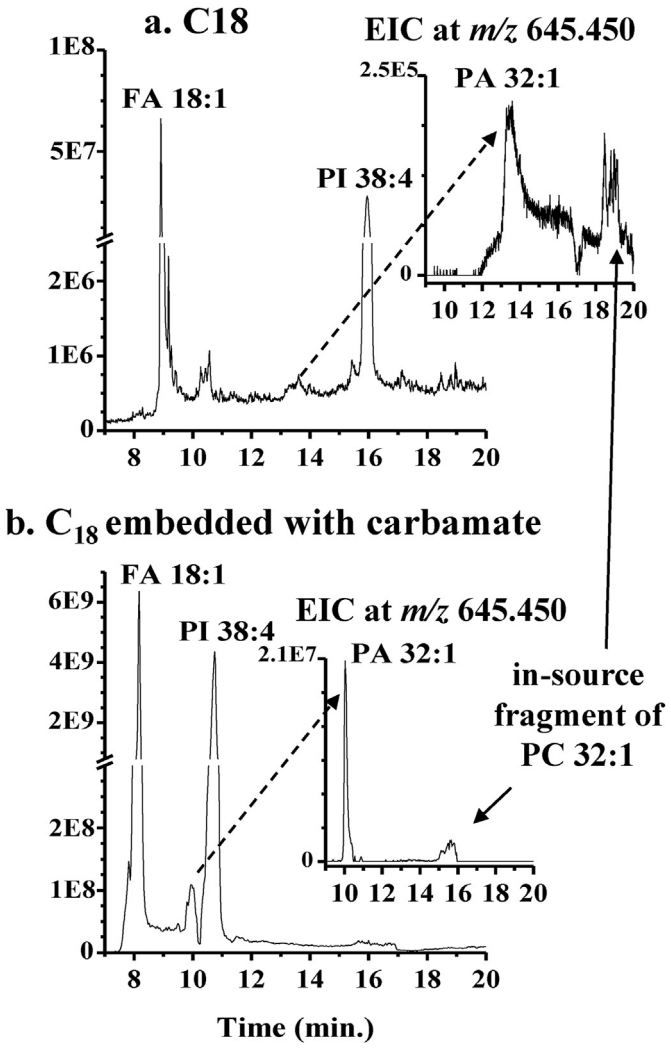

Fig. 4. Extracted ion chromatograms (EICs) of PA 32:1 (*m/z* 645.450), FA 18:1 (*m/z* 281.249), and PI 38:4 (*m/z* 885.550) from porcine brain extracts with a) conventional method using normal C18 column and b) newly developed method using carbamate-embedded C18 column. In both the panels, enlarged EICs of *m/z* 645.450 for PA 32:1 are attached.

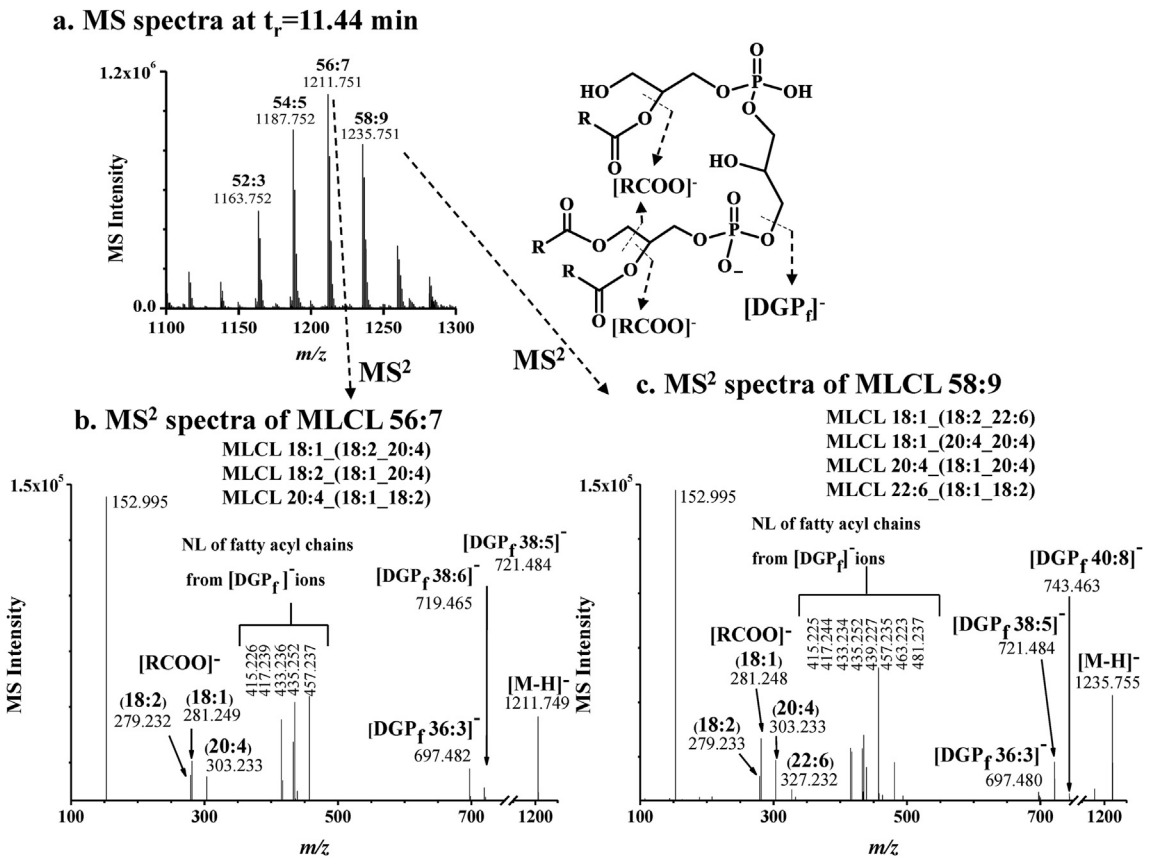

Fig. 5. a) MS spectra of a porcine brain extract at t_r = 11.44 min representing the detection of four MLCLs and MS^2 spectra of b) MLCL 56:7 and c) MLCL 58:9.

spectra of the three structural isomers of MLCL 56:7, 18:1_(18:2_20:4), 18:2_(18:1_20:4), and 20:4_(18:1_18:2) (where the parentheses represent the acyl chains attached to the same glycerol backbone of CL). Three $[DGP_f]^-$ ions originating from the three structural isomers were observed at *m/z* 697.482 ($[DGP_f\ 36:3]^-$), *m/z* 719.465 ($[DGP_f\ 38:6]^-$), and *m/z* 721.484 ($[DGP_f\ 38:5]^-$).

Specific fatty acyl chains were identified with free carboxylate ions at *m/z* 279.232, 281.249, and 303.233 as $[RCOO]^-$ produced from the acyl chains of 18:2, 18:1, and 20:4, respectively. Moreover, the NL of the fatty acyl chain from $[DGP_f]^-$ in the form of carboxyl acid $[DGP_f\text{-}RCOOH]^-$ and ketene $[DGP_f\text{-}R'CH{=}C{=}O]^-$ are shown with five fragment ions in the *m/z* range of 415.226–457.237. Similar fragment ion spectra were observed from MLCL 58:9. Fig. 5c shows a combination of fragment ion spectra of the four structural isomers, 18:1_(18:2_22:6), 18:1_(20:4_20:4), 20:4_(18:1_20:4), and 22:6_(18:1_18:2). Although this method was proven to be effective for acidic lipid analysis, accurate lipidomic quantification from cells, tissues, and urine can be very limited due to a lack of certified reference materials for each type of biological sample except plasma. For the accurate quantification of lipids from biological samples, the quantification method needs to be validated by adding the corresponding lipid standards to a representative biological matrix. However, there are few standard reference materials available for lipidomic analysis, except for the NIST SRM 1950 plasma. Therefore, the developed method was validated using this SRM.

3.3. Effectiveness of one-phase lipid extraction from plasma samples

For the effective extraction of acidic lipids, an one-phase extraction method employing a mixture of MeOH, MTBE, and $CHCl_3$ (referred to as MMC) was utilised. This method has been found to be not only effective for extracting lipids but also advantageous from the perspective of simplicity and reproducibility [32,33]. A slightly modified MMC method was carried out because the sample amount should not exceed the organic solvent capacity per recommendations in the literature [34]. Ten microliters of human plasma sample was used, and the procedure took only 20 min. Details of the extraction procedures have been described in section 2.2. Extraction recovery was measured by comparing the normalised peak area ratio of the NIST SRM 1950 plasma samples spiked with the external standard lipids before and after extraction. For comparison of the one-phase MMC method and the typical two-phase extraction method using MTBE/MeOH/H_2O, which is conventionally employed in our laboratory, five replicates of the plasma samples were prepared by spiking with the external standard lipid mixture before and after extraction. Table 1 shows the average values (n = 3) of extraction recovery of 25 lipid standards for the two extraction methods by nUHPLC–ESI-MS. Although some lipid classes including PE-P, PC-P, PE, DG, FA, and few SPs exhibited better recovery with the two-phase extraction method, the one-phase extraction method appeared to be more efficient overall. In particular, the extraction efficiencies of the acidic lipids were outstanding with the MMC method (97.3% for LPS 17:1, 97.2 for PS 17:0/17:0, 116.1 for LPA 17:0, 94.2 for PA 17:0/17:0, and 82.6 for CL-d_5 $(18:4)_4$). Moreover, the MMC method can be performed in merely 20 min. Based on this result, the one-phase MMC extraction method was found to be effective for retrieving lipids and was applied for the subsequent experiments. On the one hand, this extraction method should be used with much careful considerations. There is a possible contamination in MS instrument originated from impurities such as residual ionic salts that were not

Table 1
Comparison of one-phase (MMC) and two-phase (MTBE/MeOH/H_2O) method for lipid extraction. Extraction recovery was analysed using nUHPLC–ESI-MS by comparing the normalised peak area ratio of the standard lipids spiked to the NIST SRM 1950 plasma standard before and after extraction.

Lipid species	One-phase	Two-phases	Lipid species	One-phase	Two-phases
FA 19:0	84.8 ± 9.7	107.1 ± 16.2	PC P-18:1/18:1-d_9	85.6 ± 12.9	96.5 ± 4.7
LPC 17:1	96.9 ± 6.6	87.6 ± 3.4	PE P-18:1/18:1-d_9	88.4 ± 14.6	97.2 ± 13.3
PC 17:0/17:0	97.1 ± 7.6	99.4 ± 4.7	CL-d_5 (18:2)$_4$	82.6 ± 10.7	60.8 ± 4.4
LPE 17:1	100 ± 9.5	83.2 ± 7.9	Cer d18:1-d_7/24:1	97 ± 8.1	98.6 ± 5
PE 17:0/17:0	80.2 ± 7.1	104.6 ± 11.8	LSM d18:1-d_7	97.5 ± 7.7	75.8 ± 5.1
LPG 17:1	94.6 ± 5.4	76.5 ± 7.9	SM d18:1/17:0	93.9 ± 9.1	100.7 ± 9.8
PG 17:0/17:0	95.6 ± 7.9	93.2 ± 9	HexCer d18:1/17:0	89.2 ± 7.1	98.4 ± 5.1
LPI 17:1	94.2 ± 12.2	46.6 ± 4.8	Hex2Cer d18:1/17:0	82.6 ± 11.3	94.4 ± 9.3
PI 16:0-d_{31}/18:1	96.5 ± 7.9	99.8 ± 5.6	SulfoHexCer d18:1/17:0	87.5 ± 10.1	99.6 ± 21.4
LPS 17:1	97.3 ± 13.5	56 ± 6.7	DG-d_5 18:0_18:0	89.2 ± 9.4	101.5 ± 11.1
PS 17:0/17:0	97.2 ± 10.1	114.1 ± 1.6	TG-d_5 17:0/17:1/17:0	95.5 ± 9.9	90 ± 8.8
LPA 17:0	116.1 ± 14.2	115.7 ± 20.4	CE 17:0	108 ± 14.6	99.7 ± 7.8
PA 17:0/17:0	94.2 ± 13.7	84.6 ± 10.8			

completely removed. To avoid this issue, it would be desirable to use a minimum amount of biological sample in order to assure not only simplicity but also extraction efficiency. In contrast, the two-phase method may experience possible contamination during the retrieval of organic solvents at the liquid–liquid interface. Since the present work was focused on the enhancement of acidic lipid analysis, a thorough examination of the two extraction methods needs to be followed in a future study including the possibility of the formation of oxidative products during the extraction.

3.4. Method validation for the quantification of plasma acidic lipids

In order to evaluate the quantification efficiency of the developed method, precision and accuracy were calculated using the

Table 2
Precision and accuracy of LPS and PS standards calculated from the calibration curve. Precision was calculated as the coefficient of variance (CV) of the normalised peak area ratio for five replicate sample (n = 5) at each concentration. The normalised concentration was calculated from the linear regression of the calibration curve and accuracy was the error between the nominal and normalised concentrations.

LPS and PS standard	Nominal concentration (pmol μL^{-1})	Normalised peak area ratio (vs. IS)	Precision (CV, %)	Normalised concentration (pmol μL^{-1})	Accuracy (error, %)
LPS-d_5 15:0	0.05	0.01 ± 0.00	18.8	0.05	1.8
	0.10	0.02 ± 0.00	6.4	0.10	3.0
	0.20	0.03 ± 0.00	4.4	0.19	5.5
	0.24	0.05 ± 0.00	6.0	0.27	9.8
	4.90	0.85 ± 0.08	9.2	4.90	0.1
	7.35	1.28 ± 0.10	8.0	7.37	0.3
	14.70	2.66 ± 0.36	13.4	15.31	4.2
LPS-d_5 17:0	0.19	0.04 ± 0.00	0.6	0.19	0.0
	0.46	0.1 ± 0.01	8.4	0.45	3.8
	0.93	0.22 ± 0.01	5.9	1.02	10.0
	1.86	0.38 ± 0.02	4.6	1.79	3.5
LPS-d_5 19:0	0.18	0.03 ± 0.00	4.9	0.17	1.3
	0.22	0.04 ± 0.01	14.2	0.24	10.9
	0.88	0.14 ± 0.01	5.4	0.91	3.1
	4.41	0.62 ± 0.07	10.6	4.05	8.2
PS-d_5 17:0/14:1	0.17	0.05 ± 0.00	3.4	0.17	0.7
	0.67	0.18 ± 0.01	5.8	0.72	7.0
	3.35	0.77 ± 0.03	3.5	3.33	0.6
	5.02	1.12 ± 0.04	3.7	4.89	2.7
	10.05	2.39 ± 0.13	5.6	10.50	4.5
PS-d_5 17:0/16:1	0.26	0.06 ± 0.00	3.5	0.24	8.8
	0.32	0.09 ± 0.00	3.5	0.37	13.2
	1.29	0.29 ± 0.02	7.4	1.42	10.2
	6.46	1.29 ± 0.03	2.0	6.55	1.5
	9.68	1.78 ± 0.06	3.4	9.12	5.8
PS-d_5 17:0/18:1	0.47	0.16 ± 0.01	5.6	0.43	7.8
	0.93	0.29 ± 0.02	6.9	1.04	11.6
	1.87	0.52 ± 0.03	6.0	2.12	13.5
	9.35	2.03 ± 0.07	3.6	9.06	3.1
PS-d_5 17:0/20:3	0.24	0.05 ± 0.00	4.1	0.22	9.1
	0.30	0.07 ± 0.00	3.1	0.33	8.2
	1.21	0.27 ± 0.02	7.8	1.29	6.7
	6.05	1.25 ± 0.07	5.7	6.17	2.1
	9.07	1.77 ± 0.08	4.4	8.79	3.2
	18.15	3.53 ± 0.24	6.9	17.53	3.4
PS-d_5 17:0/22:4	0.06	0.03 ± 0.00	1.7	0.06	1.3
	0.15	0.05 ± 0.00	5.8	0.16	6.7
	0.29	0.08 ± 0.01	7.0	0.33	11.7
	0.59	0.15 ± 0.01	4.5	0.64	9.2
	2.93	0.6 ± 0.03	4.4	2.86	2.6
	4.40	0.83 ± 0.05	6.2	3.98	9.4

calibration curves. The external lipid standard mixture in Table S1 consists of 25 lipid standards added to UltimateSPLASH™ ONE, a mixture of lipid standards from 15 different classes containing various fatty acyl chains. The concentration ranges of the 25 standards in Table S1a were determined such that they are representative of the actual lipid concentrations in the human plasma, taking into account the lipid concentrations reported in inter-lab studies [35,36]. The lipid standards in Table S1b were utilised to evaluate the precision and accuracy of the various acyl chains in each lipid class. Fig. S2 shows the calibration curves established for three LPS and five PS species. Based on the curves, a good linear relationship between the normalised peak area ratio and nominal concentration of the species was observed, regardless of the difference in fatty acyl chains, although some of lipids have only four concentration levels for calibration. Table 2 presents the precision and accuracy for the SRM plasma samples spiked with LPS and PS species. As an example, with LPS-d_5 15:0, the normalised concentration for each nominal concentration was calculated from the linear regression equation of the calibration curve, $y = 0.1733x + 0.00144$, as shown in Fig. S2. Accuracy was then calculated as the error difference (%) between the normalised concentration and corresponding nominal concentration. An accuracy of 4.16% was obtained with nominal concentration of 14.70 pmol μL^{-1} and normalised concentration of 15.31 pmol μL^{-1}. Overall, the precision and accuracy for the three LPS and five PS species were below the acceptable criteria (15%) [30]. Unfortunately, although it is impossible to validate the precision and accuracy for all the acidic lipid classes due to the limited availability of standard lipids, quantitative analysis could be successfully validated for the representative acidic lipid classes, LPS and PS. Moreover, most lipid species that do not belong to acidic lipid classes including LPC, PC, LPE, PE, LPG, PG, LPI, PI, Cer, SM, DG, and TG, exhibited good precision and accuracy (<20% required for LLOQ), as shown in Table S5. Therefore, the present method developed to improve the analysis of acidic lipids was applied for the global quantification of plasma lipids.

4. Conclusion

In the present study, the efficiency of separation of acidic lipids by nUHPLC and detection with ESI-MS was enhanced by utilising carbamate-embedded C18 packing materials as the stationary phase under optimised solvent modifier conditions (0.5 mM NH_4HCO_2 + 5 mM NH_4OH). Overall, the peak tailing observed with most of the acidic lipids analysed with conventional C18 column significantly reduced and the time-based plate number values increased significantly, especially for PA 16:0/22:6, PA 16:0/18:1, PA 18:0/18:0, MLCL $(18:2)_3$, CL $(14:0)_4$, and CL $(18:1)_4$. When the method developed in this study was applied to a lipid extract from porcine brain, the capability of identifying acidic lipids was largely increased with a carbamate-embedded C18 column. Further, the present method was used to validate the quantification of NIST SRM 1950 plasma spiked with acidic lipid standards. The precision and accuracy for the quantification of various LPS and PS standards, including other lipid classes, were proven to be within the accepted criteria. The results obtained in the present study demonstrate that acidic lipid analysis in reversed-phase nUHPLC–ESI-MS/MS can be improved with the use of functionalised C18 packing material, and the peak tailing and time-based separation efficiency can be optimised. Further, the quantification process can be validated using a certified reference plasma as the matrix. Since the developed method is suitable for analysing acidic lipids as well as other lipid classes, it can be utilised for the global and targeted analysis of lipidome from biological origins with improved speed and detection capability.

CRediT authorship contribution statement

Jong Cheol Lee: Investigation, Methodology, Data curation, Writing – original draft. **Young Beom Kim:** Formal analysis. **Myeong Hee Moon:** Supervision, Writing – review & editing.

Declaration of competing interest

The authors declare that they have no known competing financial interests or personal relationships that could have appeared to influence the work reported in this paper.

Acknowledgement

Funding: This work was supported by the National Research Foundation (NRF) of Korea [grant NRF-2018R1A2A1A05019794].

Appendix A. Supplementary data

Supplementary data to this article can be found online at https://doi.org/10.1016/j.aca.2021.338573.

References

[1] J.F. Brouwers, E.A. Vernooij, A.G. Tielens, L.M. van Golde, Rapid separation and identification of phosphatidylethanolamine molecular species, J. Lipid Res. 40 (1999) 164–169.
[2] M.R. Wenk, The emerging field of lipidomics, Nat. Rev. Drug Discov. 4 (2005) 594–610.
[3] F. Hoshino, F. Sakane, Polyunsaturated fatty acid-containing phosphatidic acids selectively interact with L-lactate dehydrogenase A and induce its secondary structural change and inactivation, Bba-Mol Cell Biol L 1865 (2020).
[4] S.C. Kim, X. Wang, Phosphatidic acid: an emerging versatile class of cellular mediators, Essays Biochem. 64 (2020) 533–546.
[5] N. Kocherginsky, Acidic lipids, H(+)-ATPases, and mechanism of oxidative phosphorylation. Physico-chemical ideas 30 years after P. Mitchell's Nobel Prize award, Prog. Biophys. Mol. Biol. 99 (2009) 20–41.
[6] A.G. Buckland, D.C. Wilton, Anionic phospholipids, interfacial binding and the regulation of cell functions, Bba-Mol Cell Biol L 1483 (2000) 199–216.
[7] M.P. Muller, T. Jiang, C. Sun, M.Y. Lihan, S. Pant, P. Mahinthichaichan, A. Trifan, E. Tajkhorshid, Characterization of lipid-protein interactions and lipid-mediated modulation of membrane protein function through molecular simulation, Chem. Rev. 119 (2019) 6086–6161.
[8] E.E. Kooijman, D.P. Tieleman, C. Testerink, T. Munnik, D.T. Rijkers, K.N. Burger, B. De Kruijff, An electrostatic/hydrogen bond switch as the basis for the specific interaction of phosphatidic acid with proteins, J. Biol. Chem. 282 (2007) 11356–11364.
[9] M.A. Zhukovsky, A. Filograna, A. Luini, D. Corda, C. Valente, Phosphatidic acid in membrane rearrangements, FEBS Lett. 593 (2019) 2428–2451.
[10] C.L. Stace, N.T. Ktistakis, Phosphatidic acid- and phosphatidylserine-binding proteins, Bba-Mol Cell Biol L 1761 (2006) 913–926.
[11] H.L. Scott, F.A. Heberle, J. Katsaras, F.N. Barrera, Phosphatidylserine asymmetry promotes the membrane insertion of a transmembrane helix, Biophys. J. 116 (2019) 1495–1506.
[12] J.C. Lee, J.S. Yang, M.H. Moon, Simultaneous relative quantification of various polyglycerophospholipids with isotope-labeled methylation by nanoflow ultrahigh performance liquid chromatography-tandem mass spectrometry, Anal. Chem. 91 (2019) 6716–6723.
[13] R. Taguchi, J. Hayakawa, Y. Takeuchi, M. Ishida, Two-dimensional analysis of phospholipids by capillary liquid chromatography/electrospray ionization mass spectrometry, J. Mass Spectrom. 35 (2000) 953–966.
[14] S. Abreu, A. Solgadi, P. Chaminade, Optimization of normal phase chromatographic conditions for lipid analysis and comparison of associated detection techniques, J. Chromatogr. A 1514 (2017) 54–71.
[15] T. Cajka, J.T. Smilowitz, O. Fiehn, Validating quantitative untargeted lipidomics across nine liquid chromatography-high-resolution mass spectrometry platforms, Anal. Chem. 89 (2017) 12360–12368.
[16] E. Cifkova, M. Holcapek, M. Lisa, M. Ovcacikova, A. Lycka, F. Lynen, P. Sandra, Nontargeted quantitation of lipid classes using hydrophilic interaction liquid chromatography-electrospray ionization mass spectrometry with single internal standard and response factor Approach, Anal. Chem. 84 (2012) 10064–10070.
[17] A. Triebl, M. Trotzmuller, A. Eberl, P. Hanel, J. Hartler, H.C. Kofeler, Quantitation of phosphatidic acid and lysophosphatidic acid molecular species using hydrophilic interaction liquid chromatography coupled to electrospray ionization high resolution mass spectrometry, J. Chromatogr. A 1347 (2014) 104–110.

[18] E. Cifkova, R. Hajek, M. Lisa, M. Holcapek, Hydrophilic interaction liquid chromatography-mass spectrometry of (lyso)phosphatidic acids, (lyso)phosphatidylserines and other lipid classes, J. Chromatogr. A 1439 (2016) 65–73.
[19] H. Ogiso, T. Suzuki, R. Taguchi, Development of a reverse-phase liquid chromatography electrospray ionization mass spectrometry method for lipidomics, improving detection of phosphatidic acid and phosphatidylserine, Anal. Biochem. 375 (2008) 124–131.
[20] O.L. Knittelfelder, B.P. Weberhofer, T.O. Eichmann, S.D. Kohlwein, G.N. Rechberger, A versatile ultra-high performance LC-MS method for lipid profiling, J. Chromatogr. B 951 (2014) 119–128.
[21] N. Danne-Rasche, C. Coman, R. Ahrends, Nano-LC/NSI MS refines lipidomics by enhancing lipid coverage, measurement sensitivity, and linear dynamic range, Anal. Chem. 90 (2018) 8093–8101.
[22] S. Fekete, J. Schappler, J.L. Veuthey, D. Guillarme, Current and future trends in UHPLC, Trac. Trends Anal. Chem. 63 (2014) 2–13.
[23] E.T. Gangl, M. Annan, N. Spooner, P. Vouros, Reduction of signal suppression effects in ESI-MS using a nanosplitting device, Anal. Chem. 73 (2001) 5635–5644.
[24] G.B. Lee, J.C. Lee, M.H. Moon, Plasma lipid profile comparison of five different cancers by nanoflow ultrahigh performance liquid chromatography-tandem mass spectrometry, Anal. Chim. Acta 1063 (2019) 117–126.
[25] J.Y. Eum, G.B. Lee, S.S. Yi, I.Y. Kim, J.K. Seong, M.H. Moon, Lipid alterations in the skeletal muscle tissues of mice after weight regain by feeding a high-fat diet using nanoflow ultrahigh performance liquid chromatography-tandem mass spectrometry, J. Chromatogr. B 1141 (2020) 122022.
[26] J.S. Yang, J.Y. Kim, J.C. Lee, M.H. Moon, Investigation of lipidomic perturbations in oxidatively stressed subcellular organelles and exosomes by asymmetrical flow field-flow fractionation and nanoflow ultrahigh performance liquid chromatography-tandem mass spectrometry, Anal. Chim. Acta 1073 (2019) 79–89.
[27] K.W. Phinney, G. Ballihaut, M. Bedner, B.S. Benford, J.E. Camara, S.J. Christopher, W.C. Davis, N.G. Dodder, G. Eppe, B.E. Lang, S.E. Long, M.S. Lowenthal, E.A. McGaw, K.E. Murphy, B.C. Nelson, J.L. Prendergast, J.L. Reiner, C.A. Rimmer, L.C. Sander, M.M. Schantz, K.E. Sharpless, L.T. Sniegoski, S.S.C. Tai, J.B. Thomas, T.W. Vetter, M.J. Welch, S.A. Wise, L.J. Wood, W.F. Guthrie, C.R. Hagwood, S.D. Leigh, J.H. Yen, N.F. Zhang, M. Chaudhary-Webb, H.P. Chen, Z. Fazili, D.J. LaVoie, L.F. McCoy, S.S. Momin, N. Paladugula, E.C. Pendergrast, C.M. Pfeiffer, C.D. Powers, D. Rabinowitz, M.E. Rybak, R.L. Schleicher, B.M.H. Toombs, M. Xu, M. Zhang, A.L. Castle, Development of a standard reference material for metabolomics Research, Anal. Chem. 85 (2013) 11732–11738.
[28] J.P. Koelmel, N.M. Kroeger, C.Z. Ulmer, J.A. Bowden, R.E. Patterson, J.A. Cochran, C.W.W. Beecher, T.J. Garrett, R.A. Yost, LipidMatch: an automated workflow for rule-based lipid identification using untargeted high-resolution tandem mass spectrometry data, BMC Bioinf. 18 (2017).
[29] C.H. Yao, G.Y. Liu, K. Yang, R.W. Gross, G.J. Patti, Inaccurate quantitation of palmitate in metabolomics and isotope tracer studies due to plastics, Metabolomics (2016) 12.
[30] U.S. Department, Of Health and Human Services Food and Drug Administration, 2018. Bioanalytical Method Validation, https://www.fda.gov/media/70858/download.
[31] J.C. Lee, J.S. Yang, M.H. Moong, Simultaneous relative quantification of various polyglycerophospholipids with isotope-labeled methylation by nanoflow ultrahigh performance liquid chromatography-tandem mass spectrometry, Anal. Chem. 91 (2019) 6716–6723.
[32] R.M. Pellegrino, A. Di Veroli, A. Valeri, L. Goracci, G. Cruciani, LC/MS lipid profiling from human serum: a new method for global lipid extraction, Anal. Bioanal. Chem. 406 (2014) 7937–7948.
[33] A. Gil, W.X. Zhang, J.C. Wolters, H. Permentier, T. Boer, P. Horvatovich, M.R. Heiner-Fokkema, D.J. Reijngoud, R. Bischoff, One- vs two-phase extraction: re-evaluation of sample preparation procedures for untargeted lipidomics in plasma samples, Anal. Bioanal. Chem. 410 (2018) 5859–5870.
[34] M. Holcapek, G. Liebisch, K. Ekroos, Lipidomic analysis, Anal. Chem. 90 (2018) 4249–4257.
[35] B. Burla, M. Arita, M. Arita, A.K. Bendt, A. Cazenave-Gassiot, E.A. Dennis, K. Ekroos, X.L. Han, K. Ikeda, G. Liebisch, M.K. Lin, T.P. Loh, P.J. Meikle, M. Oresic, O. Quehenberger, A. Shevchenko, F. Torta, M.J.O. Wakelam, C.E. Wheelock, M.R. Wenk, MS-based lipidomics of human blood plasma: a community-initiated position paper to develop accepted guidelines, J. Lipid Res. 59 (2018) 2001–2017.
[36] J.A. Bowden, A. Heckert, C.Z. Ulmer, C.M. Jones, J.P. Koelmel, L. Abdullah, L. Ahonen, Y. Alnouti, A.M. Armando, J.M. Asara, T. Bamba, J.R. Barr, J. Bergquist, C.H. Borchers, J. Brandsma, S.B. Breitkopf, T. Cajka, A. Cazenave-Gassiot, A. Checa, M.A. Cinel, R.A. Colas, S. Cremers, E.A. Dennis, J.E. Evans, A. Fauland, O. Fiehn, M.S. Gardner, T.J. Garrett, K.H. Gotlinger, J. Han, Y.Y. Huang, A.H.P. Neo, T. Hyotylainen, Y. Izumi, H.F. Jiang, H.L. Jiang, J. Jiang, M. Kachman, R. Kiyonami, K. Klavins, C. Klose, H.C. Kofeler, J. Kolmert, T. Koal, G. Koster, Z. Kuklenyik, I.J. Kurland, M. Leadley, K. Lin, K.R. Maddipati, D. McDougall, P.J. Meikle, N.A. Mellett, C. Monnin, M.A. Moseley, R. Nandakumar, M. Oresic, R. Patterson, D. Peake, J.S. Pierce, M. Post, A.D. Postle, R. Pugh, Y.P. Qiu, O. Quehenberger, P. Ramrup, J. Rees, B. Rembiesa, D. Reynaud, M.R. Roth, S. Sales, K. Schuhmann, M.L. Schwartzman, C.N. Serhan, A. Shevchenko, S.E. Somerville, L.S. John-Williams, M.A. Surma, H. Takeda, R. Thakare, J.W. Thompson, F. Torta, A. Triebl, M. Trotzmuller, S.J.K. Ubhayasekera, D. Vuckovic, J.M. Weir, R. Welti, M.R. Wenk, C.E. Wheelock, L.B. Yao, M. Yuan, X.Q.H. Zhao, S.L. Zhou, Harmonizing lipidomics: NIST interlaboratory comparison exercise for lipidomics using SRM 1950-Metabolites in Frozen Human Plasma, J. Lipid Res. 58 (2017) 2275–2288.